ARCHIVES
of
FOUNDRY ENGINEERING

ISSN (2299-2944)
Volume 2025
Issue 4/2025

24 – 29

4/4

10.24425/afe.2025.155376

Published quarterly as the organ of the Foundry Commission of the Polish Academy of Sciences

Application of Elasto-optical Methods in Research on Casting Structures

M.L. Maj *, W. Stachurski
AGH University of Krakow, Faculty of Foundry Engineering, Poland
* Corresponding author: E-mail address: mmaj@agh.edu.pl

Received 02.06.25; accepted in revised form 18.07.25; available online 27.10.2025

Abstract

Verification of design conclusions using experimental methods is often employed and usually more justified than other techniques for producing machine or device components. Castings are characterized by complex shapes, varying sizes and, as a result of these factors, a variety of physical and mechanical properties. Additionally, the relatively small batches of alloys prepared for casting introduce some unintended variation in properties that affects the final characteristics and technical acceptance criteria. Therefore, it is important to consider the slightly different mechanical properties of finished castings, which may vary even within the same part due to different solidification and cooling conditions. However, despite the above-mentioned limitations, the foundry industry occupies an important position in the economy of every country, and economic indicators demonstrate the constant development of this industry. This growth is due to both low manufacturing costs and continuously improved technologies and new designs with stricter acceptance criteria for finished parts. The aim of this work was to briefly present one of the methods of experimental stress and strain analysis, namely the photoelastic method.

Keywords: Photoelastic method, Isochromatics and isoclines, Polarized light, Photoelastic coating

1. Introduction

Extensive research has been devoted to the quantification of stress states in order to design engineering components and predict their service life and failure modes during operation. Two main approaches can be distinguished: the interpretation of experimental measurements and process modeling. Most manufacturing processes induce stresses on the surface of manufactured components. These stresses can be beneficial or, in some cases, detrimental to component performance. Accurate stress determination plays a key role in understanding the complex interactions between microstructure, mechanical state, failure mode(s), and structural integrity. Furthermore, the concept of residual stress management contributes to industrial applications aimed at improving service performance and product life cycle.

Therefore, industry needs fast, efficient and modern methods for identifying and controlling residual stress states, as well as experimental studies based on model testing [1–11]. In this paper, we present the possibility of analyzing wall joints using photoelastic methods based on photoelastic models.

2. Brief Description of Photoelasticity

The photoelastic method consists of experimental and computational determination of stresses in a structural model made of transparent, isotropic material exhibiting stress-induced birefringence properties. The materials used for models are usually various types of resins (polyester, epoxy, phenol-formaldehyde, etc.), and less frequently gelatin, celluloid, and glass.

These materials are optically isotropic in stress-free and strain-free states. When a certain strain state and associated stress state occur within them, they become optically anisotropic, exhibiting stress-induced birefringence, which allows for optical study of this

state using polarized light. The models are fabricated and loaded within the limits of Hooke's law so that they conform to the basic relationships of model similarity, such as geometric similarity and load proportionality.

In classical photoelasticity studies, we use flat models. By illuminating such a loaded model with polarized light, we obtain two types of geometric patterns: isoclines and isochromatics, which are lines of identical principal stress directions σ_1 and σ_2. Using isochromatics and isoclines, we can separate these stresses using basic relationships for plane stress states. It should be noted that although photoelasticity is fundamentally an indirect method in which we conduct research on models, it also allows for direct research on actual structures using optically sensitive coatings. This is the photoelastic coating method, in which polarized light passes twice through a birefringent layer, thus doubling the number of isochromatics. While in classical photoelasticity, where light passes through the model, stress separation is mainly performed using both isochromatic and isocline fields, in the case of photoelastic coatings, the technique of oblique incidence (using only isochromatics to separate strains) is widely used.

3. Photoelastic Materials

Photoelastic materials used for model testing must meet several conditions arising from similarity theory and demonstrate good mechanical, optical and technological properties. Here are some of them:

- Optical and mechanical homogeneity
- High sensitivity to stress-induced birefringence
- Large deformations without loss of cohesion
- Linear dependence of isochromatic fringe order on stresses and deformations
- Good technological properties (machinability, bonding, casting into molds, etc.)
- Minimal edge effects and residual stresses
- Stability of physical, mechanical and optical properties during testing

During loading, it should be noted that polymeric materials exhibit some deformation immediately after unloading, which disappears after some time due to thermal motion of polymer molecules.

Table 1 below presents the properties of some polymers used in photoelasticity. The table shows that readily available epoxy resins occupy a leading position in this group. It is also worth noting the approximate nature of the given values, which is why each study must be preceded by experimental determination of the photoelastic properties of the material, represented by the material fringe value K [12–18].

Table 1.
Properties of some polymers used in elasto-optics [14, 17, 18]

Material	Young's Modulus E [MPa]	Poisson's Number ν	Photoelastic Constant K [MPa/fringe/cm]
Epoxy resins	3200–3900	0.36	1.0–1.2
CR39 resin	1800–2100	0.4	1.4–1.6
Polycarbonates	2500–3000		0.7–0.8
Polymethyl methacrylate	3100–3600	0.36	26
Rubbers	0.1–5	0.5	0.29
Soda glass	68,000	0.25	20–30

4. Models for Learning to Interpret Isochromatic Patterns

The wealth of information that each photoelastic image contains can be learned using models of known geometry. The occurrence of each isochromatic fringe is caused by the presence of forces, moments or reactions, which was demonstrated in the educational set [11] using two models.

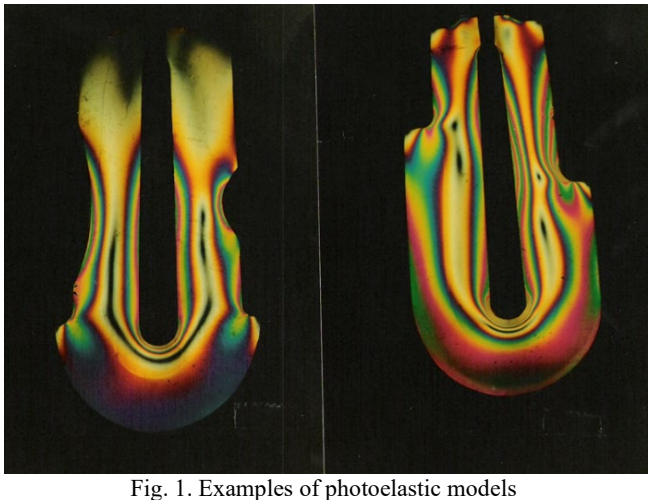

Fig. 1. Examples of photoelastic models

The bending moments in the arms of the flat model are equal, but changing their width causes stress concentration. We can perform a quick qualitative analysis based on the density of isochromatics along the edge or from the rate of their appearance with increasing load. In both models, a dark line is visible – the zero-order isochromatic fringe – which separates the tensile stress region from the compressive stress region. The isochromatic fringes intersecting the model edge allow plotting of a boundary stress graph, where one stress component (normal to the edge) equals zero, while the other is determined by multiplying the fringe order by the photoelastic model constant. The isochromatic fringe order is counted from the dark, unloaded corner or by observing the sequence of their appearance with increasing load. The model in Figure 1a is characterized by slight changes in arm thickness; therefore, almost the entire length of the inner edge has the same

fringe order of approximately 2. On the same edge of the model in Figure 1b, an uneven distribution of isochromatic fringe orders is visible, where the maximum order is 4. Clear concentration of isochromatic fringes is caused by the notches in both arms [12–18].

5. Analysis of Wall Connections in Castings

We encounter wall connections in practically every casting. Due to the fact that they form a monolithic structure, castings are very rigid and, with proper structural design, provide this desired characteristic to machine tools, housings and other machine and device components. We will first analyze this problem using flat models and then on actual cast structures, which additionally allows us to account for the specific characteristics of cast structures, rich in both favorable and unfavorable features, such as shrinkage defects [12–19].

5.1. Research on Flat Models

Walls of equal or different thicknesses can create angular, T-shaped and cross connections in castings with various thickenings, offsets, holes, etc. To ensure uniform solidification and cooling time, it is recommended that they be constructed with equal thickness. This helps reduce the tendency to create thermal nodes, where the metal solidifies last and, due to inability to replenish the deficit of liquid metal, shrinkage voids are created. During mechanical or thermal loading of casting walls with different configurations, such as a combustion engine block, a complex stress state arises that is difficult to analyze comprehensively. Several examples illustrating the distribution of isochromatic fringes in wall connections are presented below, where Figure 2a shows the stretching of two arms of a cross connection with equal arms, and Figure 2b shows unequal arms under the same loading conditions.

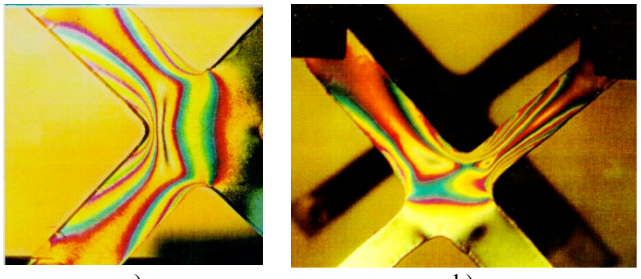

a) b)

Fig. 2. Cross connection of model walls:
a) Cross connection model of equal width with symmetrical loading of two arms (stretching effect on two arms)
b) Cross connection model in which the walls have unequal widths

The model in Figure 2 was cut from epoxy board and covered with reflective paint; then it was loaded so that tensile stresses occurred on the left edge (fringe order = 3). On the opposite edge, in the compression zone, a lower fringe order (order = 2) appeared. The zones are separated by a characteristic dark line (order = 0), which indicates the zero-order isochromatic fringe. It should be noted that the first-order isochromatic fringe is accompanied by a blue line adjacent to the red one, which always indicates a higher order on the side where it appears. This phenomenon is not observed with higher orders, where red is always adjacent to green. Under the same load, a wall of smaller width experiences greater deformations. This obvious finding is shown by the distribution of isochromatic fringes in Figure 2b, where it is also easy to identify a critical cross-section. In the central part of the connection, the first order can be observed with characteristic blue color next to the red isochromatic fringe. The first-order isochromatic fringe runs exactly through the boundary of these colors.

Shrinkage defects in thermal nodes are a common phenomenon in castings made of high-shrinkage alloys such as steel. The shape and location of defects have a major impact on joint quality in terms of stress distribution and concentration, leak-tightness, etc. Such a case is shown in Figure 3, where in case a) a round void located on the neutral axis does not pose a particular hazard, while the frequently occurring triangular shape is dangerous due to cross-section weakening and the introduction of sharp notches (case b). The images were obtained on the same model under the same load, as indicated by the location of isochromatic fringes on the tension side.

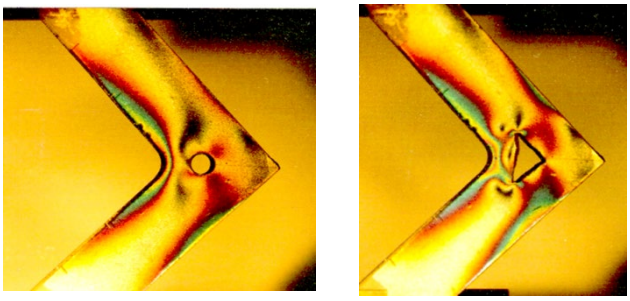

a) b)

Fig. 3. Angular connection of walls with a defect in the form of a shrinkage void of: a) round and b) triangular shape

A similar experiment was performed on a T-shaped model (Figure 4) loaded uniformly, where a) shows the loaded model without defects, b) shows the isochromatic pattern on the model with a hole made in the compressed zone, which caused the appearance of a characteristic pattern near the hole edge, c) shows the defect in the form of a triangular hole that introduced additional stress concentration in the vicinity of sharp corners.

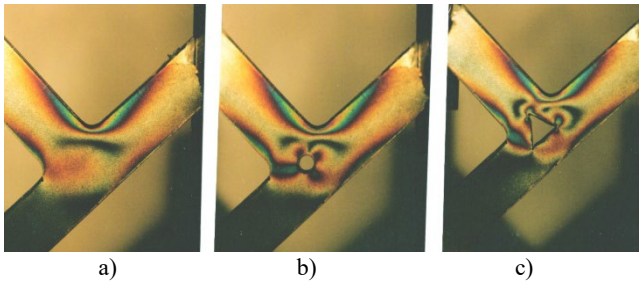

a) b) c)

Fig. 4. Influence of defect shape on the isochromatic pattern in T-shaped wall connection

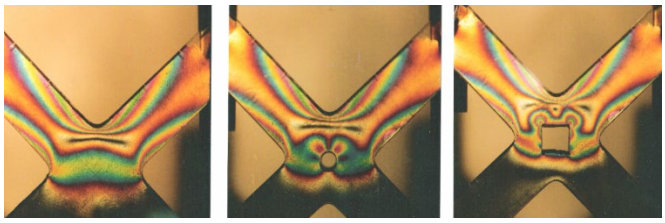

a) b) c)

Fig. 5. Similar to Figure 4 defect layout for cross connection

The equally loaded cross models of wall connections in Figure 5 refer to: a) a model without shrinkage defects, b) with a round hole introducing a characteristic isochromatic shape, c) with a square-shaped defect, clearly weakening the connection and introducing stress concentrations at the corners. All photographs in Figures 2 to 5 were taken on models cut from epoxy board, considered an isotropic material; therefore, the deformations caused by the same load, expressed in isochromatic fringes, refer only to the geometric changes of these models and thus support conclusions of a structural nature.

6. Research on Real Objects Using Photoelastic Coatings

The bonding of optically sensitive layers to a fragment of the surface of an actual casting can in some cases be treated as if this surface were covered with an equivalent number of resistance strain gauges. Figure 6 shows a fragment of a cast iron casting of a tunnel segment used for lining horizontal shallow metro tunnels. A single segment is similar to a curved ribbed plate, the lining of which can be seen in the photo as a vertical element, while the horizontal rib perpendicular to it is machined and interfaces with a similar surface of the adjacent segment (the ribs are bolted together with neoprene or lead gaskets). The load from the rock mass is transferred to the tunnel segment lining, which is responsible not only for carrying this load but also for protecting the tunnel from water. Long-term observations of underground railway operations in various countries have shown that one of the best materials for tunnel linings is gray cast iron with flake-shaped, vermicular or spherical graphite.

The next figure below shows a fragment of tests carried out on gray cast iron tunnel segments with a strength of Rm = 200 MPa. The tunnel segment fragments were covered with an optically sensitive layer 2.4 mm thick, made of epoxy resin. The epoxy adhesive contained an addition of aluminum dust. The tests were carried out after previously determining the photoelastic properties of the layer. The elements prepared in this way were loaded in an INSTRON 1273 testing machine, and the results were recorded by a reflection polariscope on color film.

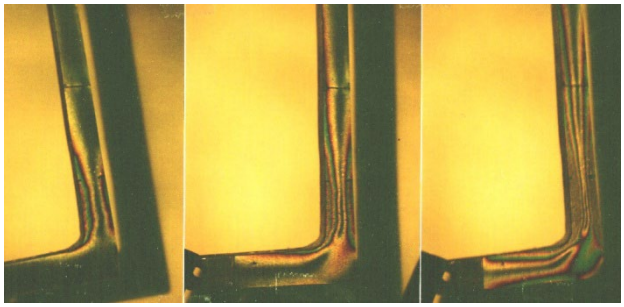

a) b) c)

Fig. 6. Isochromatic images with increasing load on the tunnel segment fragment

Based on observation of the formation of successive isochromatic fringes with increasing load, it can be assumed that the external rib of the tunnel segment (short arm at the bottom) does not deform in the same way as the longer, vertical one connected to it. More isochromatic fringes appear on the tension side, which may be related to the fact that for gray cast iron, Rm > Rc (tensile strength > compressive strength). However, in the case of angle opening, we are dealing with a complex loading case where bending occurs together with tension. Comparison of the isochromatic pattern for the same loaded, geometrically similar model from isotropic material indicates a more favorable isochromatic pattern in the model. The design change shown in Figure 7a is a more favorable solution for the angle connection, where the transition to a thinner wall is clearly defined, but with too large a difference in thickness, the thin wall is threatened by corrosion.

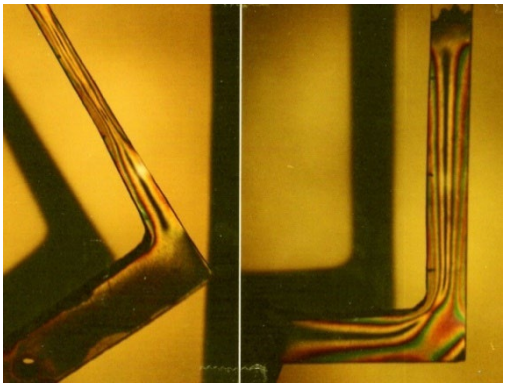

a) b)

Fig. 7: a) Construction of the casting fragment as in Figure 6, but made of more durable vermicular cast iron
b) Model of the angle connection made of Plexiglas shows a more favorable isochromatic distribution compared to Figure 6c

As mentioned earlier, the photoelastic coating method is suitable for determining deformations of the tested element beyond the elastic limit. A suitable example is shown in Figures 8 and 9. The cross connection of the thick, central rib of the tunnel segment with the thin transverse rib was stretched as indicated by the grips of the testing machine.

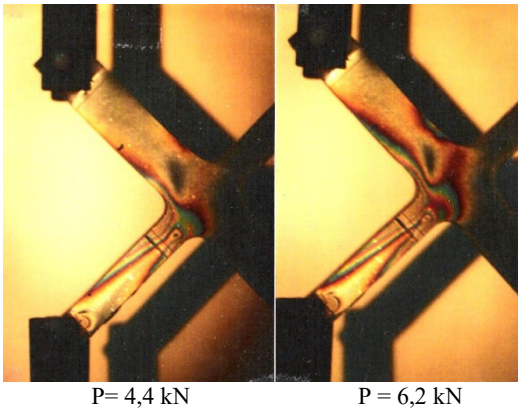

P= 4,4 kN P = 6,2 kN

Fig. 8. Isochromatics with increasing load of the cross connection of ribs of unequal thickness. At force P = 6.2 kN the elastic limit was exceeded, resulting in permanent deformation visible after load removal (Figure 9)

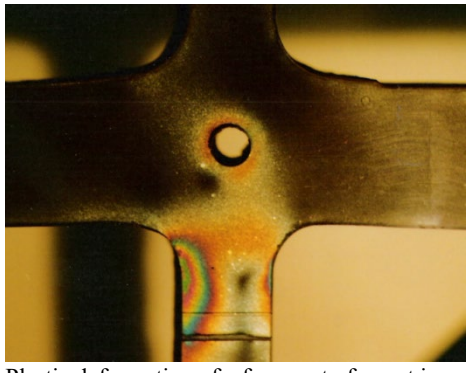

Fig. 9. Plastic deformation of a fragment of a cast iron casting locally loaded above the Rp0.2 limit

The fragment of a tunnel segment casting made of cast iron with vermicular graphite shown in Figure 9 was repeatedly loaded during various tests. At the beginning of the experiment it was covered with an optically sensitive layer 2.6 mm thick, bonded from two plates (the connection is visible as a thick, horizontal line). After the tests were completed, in which loads below the elastic limit were applied, no effects were observed on the layer. However, when the local load exceeded Rp0.2, a permanent photoelastic effect remained. In Figure 9, the 2nd order of isochromatic fringes is visible. The effect occurred on the tensile stress side. The neutral axis of the bent arm was clearly shifted toward the compressed area.

The tests of cast iron wall connections were completed by creating a hole imitating a shrinkage void. An 8 mm hole was made in the angle shown in Figure 6, and subsequent loading was carried out to show the effect of such a discontinuity on the isochromatic distribution. The results of the experiment are shown in Figure 10.

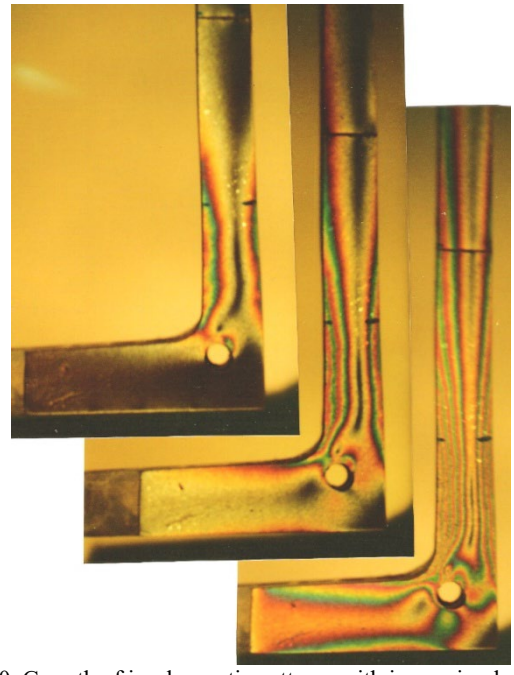

Fig. 10. Growth of isochromatic patterns with increasing load on a cast iron angle with a hole in the corner

The influence of hole proximity (defect) in a cast iron T-joint is shown in Figure 11. Due to the large difference in wall thicknesses, this example well illustrates the range of action of the cantilever beam on the region of its constraint.

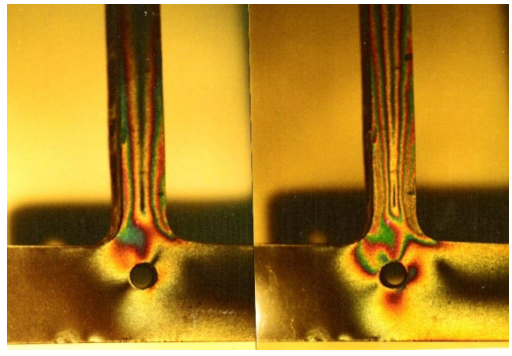

Fig. 11. The influence of the hole on the isochromatic distribution in a cast iron cantilever beam loaded with a concentrated force

7. Summary

The shape and size of castings are very diverse, from simple plates, rollers, rings or pipes, to hollow spheres, housings, rotors, etc. Their size is also characterized by a wide spectrum from small shot and fastener elements to massive rolling mill housings and other industrial objects. The problems associated with optimal strength design of castings are not always sufficiently appreciated. In cast structures, there is usually a large material reserve, the identification and removal of which without compromising the

assumed strength is an important task for engineering staff. This can be accomplished by using experimental analysis of deformations and stresses and computer-aided work of this type. In the presented article, an attempt was made to highlight the qualitative aspects of how stresses change under the influence of different configurations of wall connections, as well as under the influence of voids with shapes imitating material defects.

The figures show isochromatic fringes (colored stripes) representing the geometric loci of model points where the difference in principal stresses is constant. Dark lines on the model observed in white light indicate zero-order isochromatic fringes (no stresses), with subsequent ones being 1st order, 2nd order, etc. Each successive isochromatic fringe indicates increasing stress, corresponding to a different difference in principal stresses. Due to the specific nature of the methodology discussed in the article, providing detailed quantitative data is irrelevant.

Photoelasticity utilizes the phenomenon of stress-induced birefringence, which means that materials without birefringence become optically anisotropic under the influence of stresses and deformations, and the obtained images are superimposed on the directions of principal stresses. The scientific foundations of photoelasticity are described in a series of monographs [14–24].

References

[1] Metzger, D., Jarrett New, K. & Dantzig, J. (2001). A sand surface element for efficient modeling of residual stress in casting. *Applied Mathematical Modelling.* 25(10), 825-842. https://doi.org/10.1016/S0307-904X(01)00017-8.

[2] James, M.N., Hughes, D.J., Chen, Z., Lombard, H., Hattingh, D.G., Asquith, D., Yates, J.R. & Webster, P.J. (2007). Residual stresses and fatigue performance. *Engineering Failure Analysis.* 14(2), 384-395. https://doi.org/10.1016/j.engfailanal.2006.02.011.

[3] Rossini, N.S., Dassisti, M., Benyounis, K.Y. & Olabi, A.G. (2012). Methods of measuring residual stresses in components. *Materials & Design.* 35, 572-588. https://doi.org/10.1016/j.matdes.2011.08.022.

[4] Shet, C. & Deng, X. (2003). Residual stresses and strains in orthogonal metal cutting. *International Journal of Machine Tools and Manufacture.* 43(6), 573-587. https://doi.org/10.1016/S0890-6955(03)00018-X.

[5] Tabatabaeian, A., Ghasemi, A.R., Shokrieh, M.M., Marzbanrad, B., Baraheni M. & Fotouhi M. (2022). Residual stress in engineering materials: a review. *Advanced engineering materials.* 24(3), 2100786, 1-28. https://doi.org/10.1002/adem.202100786.

[6] Jun, T.-S. & Korsunsky, A.M. (2010). Evaluation of residual stresses and strains using the eigenstrain reconstruction method. *International Journal of Solids and Structures.* 47(13), 1678-1686. https://doi.org/10.1016/j.ijsolstr.2010.03.002.

[7] Wyatt, J.E., Berry, J.T. & Williams, A.R. (2007). Residual stresses in aluminum castings. *Journal of materials processing technology.* 191(1-3), 170-173. https://doi.org/10.1016/j.jmatprotec.2007.03.018.

[8] Carrera, E., Rodríguez, A., Talamantes, J., Valtierra, S. & Colás, R. (2007). Measurement of residual stresses in cast aluminium engine blocks. *Journal of materials processing technology.* 189(1-3), 206-210. https://doi.org/10.1016/j.jmatprotec.2007.01.023.

[9] Guan, J., Dieckhues, G.W. & Sahm, P.R. (1994) Analysis of residual stresses and cracking of γ-TiAl castings. *Intermetallics*. 2(2), 89-94. https://doi.org/10.1016/0966-9795(94)90002-7.

[10] Skarbiński, M. (1957). *Construction of Castings*. Warszawa: PWT.

[11] Training materials from Vishay.

[12] Maj, M. (2024). The formation of the strength of castings including stress and strain analysis. *Materials.* 17(11), 2484, 1-19. https://doi.org/10.3390/ma17112484.

[13] Maj, M. (2012). *Fatigue endurance of selected casting alloys.* Katowice-Gliwice*:* Archives of Foundry Engineering.

[14] Wolna, M. (1993). *Elastooptic Materials*. Warsaw: Wydawnictwo Naukowe PWN.

[15] Jakubowicz, A., Orłoś, Z. (1972), *Strength of Materials.* Warszawa: Wydawnictwa Naukowo-Techniczne.

[16] Orłoś, Z. (1977). *Experimental Analysis of Deformations and Stresses* [*Doświadczalna analiza odkształceń i naprężeń.*]; Warszawa: PWN. (in Polish)

[17] Stachurski, W., Siemieniec, A. (2005). *Structural Studies of Castings Using Elastooptics Methods.* Kraków: WN AKAPIT.

[18] Siemieniec, A. (1977). *Elastooptics.* Kraków: Wydawnictwo AGH. (in Polish).

[19] Zandman, F., Redner, S., & Dally, J. W. (1977). *Photoelastic coatings* (SESA Monograph No. 3). Iowa State University Press.

[20] Ulutan, D., Ulutan, B., Erdem, A. & Lazoglu, I. (2007). Analytical modelling of residual stresses in machining. *Journal of Materials Processing Technology*. 183(1), 77-87. https://doi.org/10.1016/j.jmatprotec.2006.09.032.

[21] Raptis, K.G., Costopoulos, Th.N., Papadopoulos, G.A. & Tsolakis, A.D. (2010). Rating of spur gear strength using photoelasticity and the finite element method. *American Journal of Engineering and Applied Sciences*. 3(1), 222-231. ISSN 1941-7020.

[22] Umezaki, E. & Terauchi, Sh. (2002). Extraction of isotropic points using simulated isoclinics obtained by photoelasticity-assisted finite element analysis. *Optics and lasers in engineering*. 38(1-2), 71-85. https://doi.org/10.1016/S0143-8166(01)00158-0.

[23] Marle Ramachandra, P., Sungar, S., Mohan Kumara, G.C. (2022). Stress analysis of a gear using photoelastic method and Finite element method. *Materials Today: Proceedings*. 65(8), 3820-3828. https://doi.org/10.1016/j.matpr.2022.06.579.

[24] Corby Jr, T.W., Nickola Wayne, E. (1997). Residual strain measurement using photoelastic coatings. *Optics and Lasers in Engineering*. 27(1), 111-123. https://doi.org/10.1016/S0143-8166(95)00012-7.